Aggregation of Colloidal Particles in the Presence of Hydrophobic Anions: Importance of Attractive Non-DLVO Forces

Cao, Tianchi; Trefalt, Gregor; Borkovec, Michal

How to cite

CAO, Tianchi, TREFALT, Gregor, BORKOVEC, Michal. Aggregation of Colloidal Particles in the Presence of Hydrophobic Anions: Importance of Attractive Non-DLVO Forces. In: Langmuir, 2018, vol. 34, n° 47, p. 14368–14377. doi: 10.1021/acs.langmuir.8b03191

This publication URL: https://archive-ouverte.unige.ch/unige:111925
Publication DOI: 10.1021/acs.langmuir.8b03191

Revised, October 31, 2018

Published in Langmuir, 2018, 34, 14368-14377

DOI: 10.1021/acs.langmuir.8b03191

Aggregation of colloidal particles in the presence of hydrophobic anions:

Importance of attractive non-DLVO forces

Tianchi Cao, Gregor Trefalt, Michal Borkovec*

Department of Inorganic and Analytical Chemistry, University of Geneva, Sciences II,

30 Quai Ernest-Ansermet, 1205 Geneva, Switzerland

*Corresponding author: michal.borkovec@unige.ch (email)

Abstract

Aqueous suspensions of amidine latex (AL) and sulfate latex (SL) particles containing sodium tetraphenylborate and NaCl are studied with electrokinetic and time-resolved light scattering techniques. In monovalent salt solutions, AL is positively charged, while SL negatively. Electrophoretic mobility measurements demonstrate that adsorption of tetraphenylborate anions leads to a charge reversal of the AL particles. At higher concentrations, both types of particles accumulate negative charge. For the AL particles, the charge reversal leads to a narrow fast aggregation region and an intermediate regime of slow aggregation. For the SL particles, the intermediate slow regime is also observed. These aspects can be explained with classical theory of Derjaguin, Landau, Verwey, and Overbeek (DLVO). Another regime of fast aggregation is observed at intermediate concentrations, and the existence of this regime can be rationalized by an additional attractive non-DLVO force. We suspect that this additional force is caused by surface charge heterogeneities.

Graphical Abstract

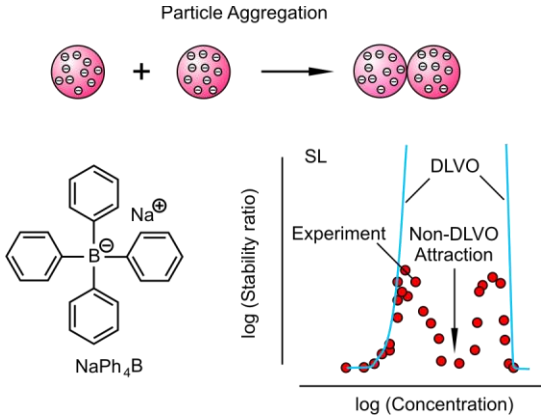

Introduction

Particle aggregation is one of the key pathways for the destabilization of colloidal particle suspensions.[1,2] Since this process is relevant in many industrial phenomena, including water treatment or papermaking, it has been studied to substantial detail in the past.[3,4] The time scale of the aggregation process is set by the formation rate of particle doublets in a dilute suspension. When the interaction between the colloidal particles is attractive, particle aggregation is fast and controlled by diffusional approach. When the interactions are repulsive, the particles must overcome an activation barrier, and therefore the particle aggregation is slow. As the transition region between the fast regimes is relatively narrow, it is normally characterized by the so-called critical coagulation concentration (CCC).

The famous theory of Derjaguin, Landau, Vervey, and Overbeek (DLVO) suggests that the interactions between the particles are governed by two main contributions, namely van der Waals and double layer forces.[1,2,5,6] For weakly charged particles and high salt levels, double layer forces are negligible and interactions are governed by attractive van der Waals forces. Under these conditions, fast aggregation is expected. For highly charged particles and lower salt levels, repulsive double layer forces become important, which induces a slowdown of the aggregation process.

This theory further stipulates that a key parameter determining the rate of colloidal aggregation is the electric diffuse layer potential, since this potential dictates the strength of the double layer forces. For small colloidal particles, the diffuse layer potential cannot be easily measured experimentally, but one can instead use the electrokinetic potential, which is also referred to as the ζ-potential. This potential can be extracted from experimentally accessible electrophoretic mobility, and such potentials have been shown to approximate diffuse layer potentials rather well.[7,8] Researchers have exploited the relation between the electrokinetic potential and colloidal aggregation rate most successfully. In many systems, the aggregation rate is governed by the electrokinetic potential, which includes effects of salt concentration as well as of charge reversal. Examples include solutions of various additives, such as, salts containing monovalent and multivalent ions, polyelectrolytes, or ionic surfactants.[9-18] Indeed, for sufficiently high salt conditions, the magnitude of the electrokinetic potential is low, and particles in colloidal suspensions aggregate rapidly. For low salt conditions, the magnitude of the potential becomes high, and slow aggregation is observed. When an additive induces a charge reversal, the electrokinetic potential goes through zero, and at this point the aggregation becomes rapid too.

Here we demonstrate that this picture is only partially valid in the case of polystyrene latex particles with different surface functionalities in the presence of tetraphenylborate (Ph_4B^-) anions. Polystyrene latex particles represent a well-studied monodisperse and spherical colloids, whose aggregation behavior can be well described by DLVO theory, definitely in the case simple monovalent and

multivalent ions.[11-13] However, the charging behavior of the particles must be known, and included through measured electrokinetic potentials.

Ph_4B^- anions and analogous tetraphenylphosphonium (Ph_4P^+) or tetraphenylarsonium (Ph_4As^+) cations are hydrophobic monovalent ions, whose salts readily dissolve in water. Such ions should be positioned on the extremes of the Hofmeister series, which classifies ions according their hydrophobicity.[19] Similarly to ionic surfactants, they strongly adsorb to hydrophobic substrates, and may induce a charge reversal.[20-22] In contrast to ionic surfactants, which are comprised of a hydrophilic charged head group and a hydrophobic tail, tetraphenyl ions bear hydrophobic phenyl groups, which are bound to the central charged ion. To our knowledge, these ions do not form micelles in aqueous solutions. For this reason, they represent interesting class of monovalent ions that are highly suitable to study effects of hydrophobic interactions on adsorption processes, electrophoretic mobility, or colloidal aggregation. While few studies are available concerning the effects of these ions on electrokinetic and diffuse layer potentials[20-23], there is basically no information concerning their effects on particle aggregation.

The present study explores the aggregation of colloidal particles in the presence of Ph_4B^- ions experimentally. We demonstrate that DLVO theory, which relies on electrokinetic data, is insufficient even to qualitatively rationalize the aggregation behavior in such systems. We thus argue that additional attractive non-DLVO forces, which appear similar to the ones recently reported in direct force measurements[7,23-25], are the cause for the presence of an additional fast aggregation region.

Experimental and Methods

Materials. Two types of functionalized, surfactant-free polystyrene particles (Invitrogen Corporation) were used, namely amidine latex (AL) and sulfate latex (SL). The average particle radius and their polydisperisty as determined by the manufacturer with transmission electron microscopy are given in Table 1. The particle suspensions were purified by dialysis in Milli-Q water (Millipore) for about a week, until the conductivity of water was below 80 mS/m. Polyvinylidene fluoride and cellulose ester membranes were used to dialyze the amidine and sulfate latex suspensions, respectively. The same AL particles were already used in previous studies.[26,27]

Analytical grade sodium tetraphenylborate, $NaPh_4B$, and sodium chloride, NaCl, both from Sigma-Aldrich were dissolved with Milli-Q water and the pH was adjusted to 4.0 with HCl. Prior to use, the $NaPh_4B$ stock solution of a concentration 1.2 M was left to stand overnight, then centrifuged at 18'000 *g* during 30 min, and then filtered with a 0.1 μm syringe filter (Millipore). The latter steps were needed to free the salt solution from particulate impurities.

Electrophoresis. ZetaSizer Nano ZS (Malvern Instruments) was used to measure the electrophoretic mobility of the particles in aqueous suspensions containing different salt concentrations. Suspensions used in the experiments prepared by first mixing stock solutions of NaCl and $NaPh_4B$ stock solution with Milli-Q water to obtain the desired concentrations. Immediately prior the measurement, a stock suspension of the latex particles was added and the suspension was mixed. The final particle concentrations used were 5 mg/L for both particles. This mass concentration corresponds to a number concentration of 3.4×10^{14} m^{-3} for AL and 7.1×10^{14} m^{-3} for SL. The measured electrophoretic mobility was converted to electrokinetic potentials (ζ-potential) by means of the O'Brien and White model.[28]

Light scattering. Particle aggregation was measured with a light scattering goniometer equipped with eight fiber optic detectors (ALV/CGS-8F) and a solid-state laser with a wavelength of 532 nm. The experiments were performed in borosilicate cuvettes. The cuvettes were cleaned in hot piranha solution, which is a mixture of 96% H_2SO_4 and 30% H_2O_2 of a volume ratio of 3:1, then thoroughly washed with Milli-Q water, and dried in a dust-free oven at 60 °C. The signal was accumulated for 20 s and correlation functions were analyzed with a second-order cumulant fit. The experiments were carried out in the early stages of the aggregation process, and this condition was ensured by verifying that the apparent hydrodynamic radius did not increase more than 30% during the experiment.

Absolute aggregation rates were determined in particle suspensions by time-resolved simultaneous static and dynamic light scattering (SSDLS). The suspensions were adjusted to pH 4.0 and contained NaCl at a concentration of 600 mM. The particles concentrations were 0.62 mg/L (4.2×10^{13} m^{-3}) for AL and 0.69 mg/L (9.8×10^{13} m^{-3}) for SL. The apparent static $\Sigma = I(0)^{-1}\, dI/dt\big|_{t\to 0}$ and dynamic $\Delta = R(0)^{-1}\, dR/dt\big|_{t\to 0}$ aggregation rates were extracted from the initial dependence of the scattering intensity I and the apparent hydrodynamic radius R on time t. The absolute rates were then obtained by fitting the linear relation between these two quantities[29,30]

$$\Sigma = \left(1 - \frac{1}{\alpha}\right)\Delta - kN_0 \qquad (1)$$

where N_0 is the initial particle number density and α is the hydrodynamic factor. The experimental results are shown in Fig. 1 and the resulting rate coefficients are given in Table 1. The fitted hydrodynamic factors agree within experimental error with the theoretical value of 1.38 reported earlier.[29] For the AL particles, the measured rate coefficient is the same as the one published earlier within experimental error.[26,27] For other conditions, the apparent dynamic rate was measured at a scattering angle of 90°, from which the stability ratio was extracted. The suspensions used in the latter experiments were prepared in the same way as for the electrophoresis.

Static light scattering (SLS) was used to extract accurate particle radii and polydispersities. Scattering intensity was measured as a function of the scattering angle in particle suspensions adjusted to pH 4.0 and without added NaCl at particle concentrations 1.4 mg/L (9.5×10^{14} m^{-3}) for AL and 2.7 mg/L (3.8×10^{14} m^{-3}) for SL. The scattering profile was fitted to Mie theory including particle polydispersity and back reflection as described earlier.[26,27] SLS was also used to determine the particle concentrations of the dialyzed suspensions. These concentrations were determined by comparing the scattering intensities of dialyzed suspensions with the ones of the original suspensions, where the concentrations were known. Particle radius was also measured by dynamic light scattering (DLS) at a scattering angle of 90° in particle suspensions without added NaCl adjusted to pH 4.0 at particle concentrations 5.0 mg/L for both types of particles. The measured radii and polydispersities are summarized in Table 1 and they agree well with the ones reported by the manufacturer. The slightly larger radii measured by DLS are likely caused by polydispersity effects.

Model Calculations. The aggregation rate coefficient *k* of doublet formation of monodisperse spherical particles can be calculated by finding the steady-state solution of the forced diffusion equation. This resulting expression involves the interaction potential $V(h)$ acting between the particles, where *h* is the smallest surface separation, and can be written as[1,2]

$$k = \frac{4}{3\eta R\beta}\left[\int_0^\infty \frac{B(h)}{(2R+h)^2}\exp[\beta V(h)]\,dh\right]^{-1} \tag{2}$$

where η is the shear viscosity, *R* the particle radius , $\beta = 1/(k_B T)$ the inverse thermal energy, and $B(h)$ is the hydrodynamic resistance function. We use η = 8.90×10^{-4} Pas as appropriate for water at 25°C. We further denote by *T* the absolute temperature, by k_B the Boltzmann constant, and the hydrodynamic function is approximated as[1,2]

$$B(h) = \frac{6h^2 + 13hR + 2R^2}{6h^2 + 4hR} \tag{3}$$

Instead of the rate coefficient, we normally report the stability ratio defined as

$$W = \frac{k_{fast}}{k} \tag{4}$$

where k_{fast} is the rate coefficient under fast aggregation conditions as realized at high salt concentration.

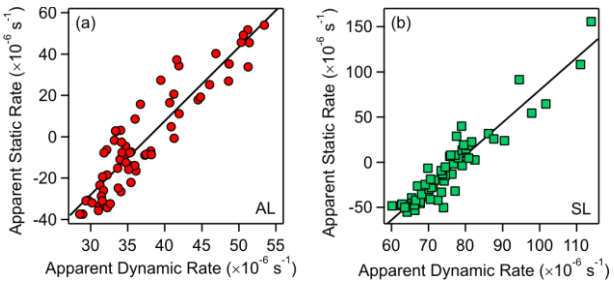

Figure 1. Scatter plots of apparent static rates versus the apparent dynamic rates measured by time-resolved simultaneous static and dynamic light scattering (SSDLS) in 600 mM NaCl and pH 4.0 to extract fast aggregation rate coefficients, which are given in Table 1. (a) Amidine latex, (b) sulfate latex.

Table 1. Selected properties of the latex particles used

Particles	Radius (nm)			Polydispersity (CV, %)		ζ-Potential[d] (mV)	CCC[e] (mM)	Fast rate[f] k_{fast} ($\times 10^{-18}$ m^3/s)
	TEM[a]	SLS[b]	DLS[c]	TEM[a]	SLS[b]			
Amidine Latex (AL)	150	149±2	153±3	5.7	6.5±0.9	+48±2	152±9	3.1±0.2
Sulfate Latex (SL)	125	117±2	123±2	3.1	7.2±0.7	–50±1	149±2	2.9±0.2

[a]Measured by transmission electron microscopy (TEM) by the manufacturer. [b]Measured by static light scattering (SLS). [c]Measured by dynamic light scattering (DLS). [d]Electrokinetic potential measured by electrophoresis without added salt at pH 4.0. [e]Critical coagulation concentration (CCC) in NaCl solutions at pH 4.0. [f]Measured absolute fast aggregation rate coefficients in 600 mM NaCl solutions of pH 4.0.

The interaction potential profile $V(h)$ between two particles is obtained by integrating the interaction energy $W(h)$ in the plate-plate geometry within the Derjaguin approximation[1,2]

$$V(h) = \pi R \int_h^\infty W(h')\, dh' \tag{5}$$

We assume that this interaction has three additive contributions, namely

$$W = \overbrace{W_{\mathrm{vdW}} + W_{\mathrm{dl}}}^{\mathrm{DLVO}} + W_{\mathrm{att}} \tag{6}$$

where W_{vdW} denotes the contribution due to van der Waals interaction, W_{dl} due to the double layer, and W_{att} is an additional attractive interaction.

The two DLVO contributions W_{vdW} and W_{dl} are calculated as follows. Van der Waals interactions are obtained from the non-retarded expression[1,2]

$$W_{\mathrm{vdW}} = -\frac{H}{12\pi h^2} \tag{7}$$

where *H* is the Hamaker constant. The double layer interaction is inferred from the PB equation for a monovalent electrolyte between two identical and homogeneously charged plates. The electric potential profile $\psi(x)$ is a function of the position *x* and satisfies the equation

$$\frac{d^2\psi}{dx^2} = \frac{2ec}{\varepsilon_0 \varepsilon} \sinh(\beta e \psi) \tag{8}$$

where *e* is the elementary charge, ε_0 is the permittivity of vacuum and ε is the dielectric constant of water. The latter parameter is taken ε = 80 throughout, as applicable for water at 25°C. The PB equation is solved numerically between the two charged plated located at $x = \pm h/2$ subject to the constant charge (CC) and constant potential (CP) boundary conditions. In either case, the charge of the isolated surface is characterized by its electric potential ψ_{D}, referred to as the diffuse layer potential. The swelling pressure Π is then evaluated from the value of the electric potential at the midplane $\psi_{\mathrm{m}} = \psi(0)$ as

$$\Pi = 2k_{\mathrm{B}}T[\cosh(\beta e \psi_{\mathrm{m}}) - 1] \tag{9}$$

Finally, the interaction potential between the plates is found by integrating the pressure profile, namely

$$W_{\mathrm{dl}}(h) = \int_{h}^{\infty} \Pi(h')\, dh' \tag{10}$$

Further details on similar PB calculations can be found in the literature.[1,2,27]

While DLVO theory stipulates that interactions can be approximated with the first two terms, an additional attractive non-DLVO force will be considered here. This additional contribution is modeled by an exponential function, namely

$$W_{\mathrm{att}} = -Ae^{-qh} \tag{11}$$

where $A > 0$ is the amplitude of the interaction and q^{-1} its decay length. Such exponential attractive forces were proposed theoretically to originate from patch-charge heterogeneities or hydrophobic interactions.[31,32] In system containing multivalent or hydrophobic ions, direct force measurements equally reveal the existence of exponential non-DLVO forces with a decay length around 1 nm.[7,23,24] Patch-charge interactions were also invoked to interpret forces acting between charged surfaces with adsorbed polyelectrolytes of oppositely charge.[33-35] However, the respective length scales are substantially larger in the latter systems.

Results and discussion

This article presents measurements of particle aggregation rates and of electrophoretic mobilities for submicron amidine latex (AL) and sulfate latex (SL) particles in aqueous solutions containing sodium tetraphenylborate ($NaPh_4B$) and NaCl. All experiments were carried out in aqueous solutions adjusted to pH 4.0 and at a temperature of 25°C. In monovalent salt solutions, the AL particles are positively charged, while the SL particles negatively. Further properties of these particles are summarized in Table 1. As the Ph_4B^- anion is hydrophobic, it strongly adsorbs on the latex particle surfaces. This adsorption process induces an accumulation of negative charge on the particles, and the accumulated charge modifies the aggregation behavior substantially. Further analysis of these results and comparison with model calculations based on DLVO theory reveals that additional attractive non-DLVO forces are active and modify the aggregation behavior further.

Charging behavior. Electrophoresis measurements were performed to study the influence of Ph_4B^- ions on the charging behavior of the AL and SL particles. The electrophoretic mobilities were converted to electrokinetic potentials (ζ-potentials) and their dependence on the Ph_4B^- concentration is shown in Fig. 2. The effect of adding NaCl was equally studied.

Figure 2a shows the measured electrokinetic potentials for AL particles. At very low concentrations of Ph_4B^-, the potentials are positive and they reflect the positive charge caused by the cationic amidine groups at the AL particle surface. As the concentration is increased, Ph_4B^- anions adsorb to the positively charged AL particles, and cause an accumulation of negative charge. This accumulation first leads to charge neutralization at a concentration of 0.030±0.005 mM, and subsequently to a pronounced charge reversal. The electrokinetic potential reaches a minimum around a concentration of 10 mM, and then the potential increases due to screening. Addition of the indifferent NaCl electrolyte reduces the magnitude of the potentials, but otherwise leaves the features unchanged. However, when one calculates the respective electrokinetic charge by means of the Grahame equation, one observe that the magnitude of the charge density slightly increases with increasing NaCl concentration. This trend suggest that the presence of salt promotes the adsorption of Ph_4B^- anions. However, the position of the charge neutralization point remains the same, indicating that this effect is relatively weak.

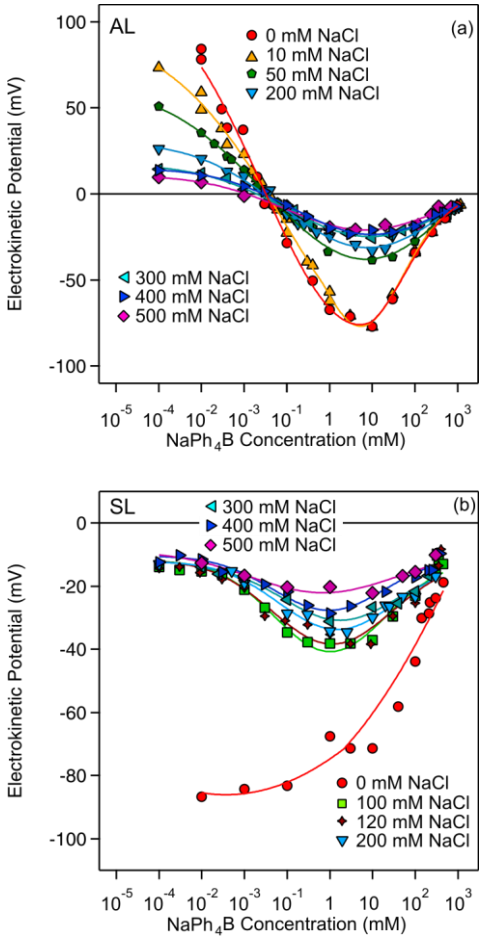

Figure 2. Electrokinetic potentials (ζ-potentials) measured by electrophoresis versus the concentration of $NaPh_4B$ and different concentrations of added NaCl at pH 4.0. Solid lines are empirical interpolating functions used in the model calculations. (a) Amidine latex, (b) sulfate latex.

These observations concerning the charge reversal are in line with recent electrophoresis experiments with negatively charged latex particles in the presence of Ph_4P^+ cations.[21,22] These authors also observe a charge neutralization point at Ph_4P^+ concentrations in the range 0.5–3 mM and they do not report any shifts of this point upon addition of KCl. Direct force measurements between sulfate particles in the presence of Ph_4As^+ at pH 4.0 without added salt reveal that the charge neutralization point is located at somewhat lower concentration, near 0.2 mM. These publications and our findings all suggest that monovalent tetraphenyl ions systematically induce a charge reversal of oppositely charged latex particles, and that this reversal occurs in the mM concentration range or below.

Similar charge reversal phenomena were also observed with colloidal particles in the presence of other strongly adsorbing species. These systems include oxide particle suspensions containing oppositely charged surfactants[15,36-40] or when subject to pH variations[11,17,18], and latex particle suspensions in the presence of oppositely charged polyelectrolytes or highly charged multivalent ions.[14,16,26,41,42]

Figure 2b shows the respective electrokinetic potentials for SL particles. At very low concentrations of Ph_4B^-, the potentials are negative, as they reflect the negative charge of the anionic sulfate groups at the SL particle surface. Without added NaCl, the electrokinetic potentials increase with increasing Ph_4B^- concentration. However, as soon NaCl is being added, one observes an intermediate minimum in the electrokinetic potential, which indicates that the Ph_4B^- anions also adsorb to the negatively charged SL particles. The potentials go again through a minimum near 10 mM and they increase at higher concentrations. The latter increase is caused by screening. The electrokinetic charge shows a similar trend as for the AL particles.

The occurrence of adsorption in this like-charged situation strongly suggests that other forces than electrostatic ones are responsible for this adsorption process. These forces are probably of hydrophobic nature. The presence of the phenyl rings makes the Ph_4B^- anion hydrophobic, and the same applies to the polystyrene latex particles, and in this situation strong hydrophobic and π-π stacking interactions are likely to be present. Nevertheless, a similar accumulation of negative charge was observed for clay minerals and carbon nanotubes in the presence of sodium dodecyl sulfate by similar electrophoresis experiments.[43,44]

The adsorption of Ph_4B^- to SL particles in the like-charged situation further indicates that the same forces are responsible for the adsorption of Ph_4B^- to the AL particles in the oppositely-charged case. The fact that the main features of the electrokinetic potential do not depend on the addition of an indifferent electrolyte for both types of particles further supports the fact that effects of electrostatic forces on the adsorption process are minor. Thus we conclude that hydrophobic forces are responsible

for the strong adsorption of Ph_4B^- to both types of latex particles, irrespective of the sign of their charge.

Aggregation rates. In solutions of indifferent NaCl electrolyte, which are free of the Ph_4B^- ions, the investigated latex particles show the classical aggregation behavior. At high concentrations of indifferent salt, NaCl, the particles aggregate rapidly, and their absolute aggregation rate coefficients are summarized in Table 1. These values are typical for fast aggregation controlled by diffusion. When the NaCl concentration is being decreased, the aggregation starts to slow down, which happens below the CCC around 150 mM. This concentration marks the onset of double layer repulsion. Model calculations based on DLVO theory reveal very similar patterns. This observed behavior is typical for highly charged colloidal particles, and has been reported in numerous studies earlier.[26,45-47]

The presence of Ph_4B^- in solution profoundly modifies the aggregation rates of the AL and SL particles investigated. Figure 3 summarizes the experimentally measured stability ratios, which were calculated from the aggregation rates by means of eq. (4). The fast aggregation rate k_{fast} in this relation is the one in concentrated NaCl solution. The effect of different concentrations of NaCl on the aggregation behavior in the presence Ph_4B^- was equally investigated.

The dependence of the stability ratios of the AL particles on the Ph_4B^- concentration is shown in Fig. 3a. At very low Ph_4B^- concentrations, the particles are stable, but as the NaCl concentration is increased, the stability ratio decreases to unity, where the fast aggregation conditions are reached. As the Ph_4B^- concentration is being increased, the stability ratio decreases, and near 0.03 mM the ratio becomes unity even in the absence of NaCl. As evidenced by electrophoresis experiments, this point marks the charge neutralization point. At this point, double layer repulsion between the particles is absent, and therefore the stability ratio becomes unity. As the Ph_4B^- concentration is increased further, the stability ratio increase again strongly, mainly due to double layer repulsion. The minimum in the stability ratio widens with increasing NaCl concentration, which suggests the onset of screening effects and the importance of double forces. This minimum in the stability ratio leads to the presence of two CCCs, which are located below and above the charge neutralization point. Similar minima in the stability ratios that widen with increasing concentration of an indifferent salt were reported for many other colloidal systems undergoing a charge reversal. These systems include oxide particle suspensions containing oppositely charged surfactants[15,36,37,39] or when subject to pH variations[11,18] and latex particle suspensions in the presence of oppositely charged polyelectrolytes or highly charged multivalent ions.[14,16,26,41,42]

At very high concentrations of Ph_4B^-, the stability ratio decreases rapidly with the concentration and becomes unity for Ph_4B^- concentrations above 790±20 mM. This concentration marks the CCC due to screening, and is comparable, but higher, as the one observed in NaCl solutions (Table 1). In between

the charge neutralization point and this CCC, the stability ratios become very high for lower concentrations of NaCl. At high NaCl concentrations, on the other hand, the stability ratio is basically unity.

However, we observe an unexpected effect at intermediate NaCl and Ph_4B^- concentrations. This effect is especially prominent in solutions containing 300 mM NaCl, where an intermediate minimum in the stability ratio can be observed around 10 mM $NaPh_4B$. Moreover, for NaCl concentrations of 400 mM and 500 mM, a sharp maximum in the stability ratio in the $NaPh_4B$ concentration range of 300–400 mM is present. These features point towards the importance of an additional attractive force.

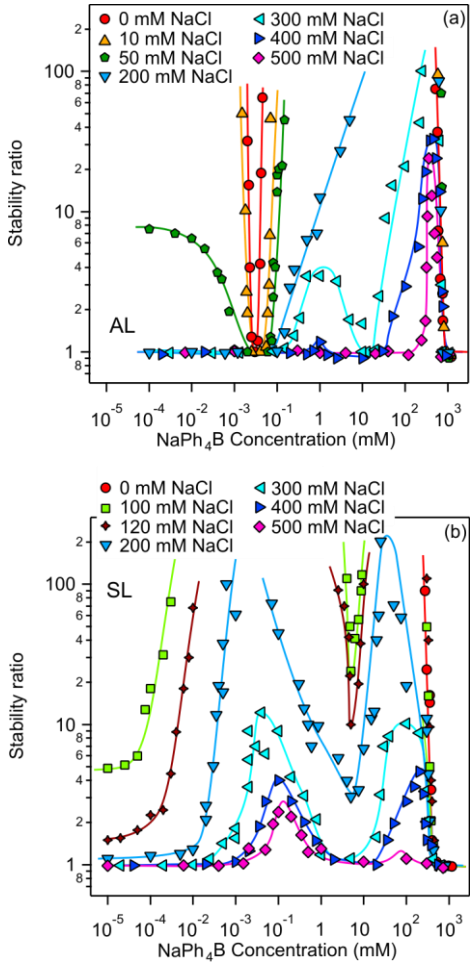

Figure 3. Stability ratios measured by time-resolved light scattering versus the concentration of $NaPh_4B$ and different concentrations of added NaCl at pH 4.0. The solid lines serve to guide the eyes. (a) Amidine latex, (b) sulfate latex.

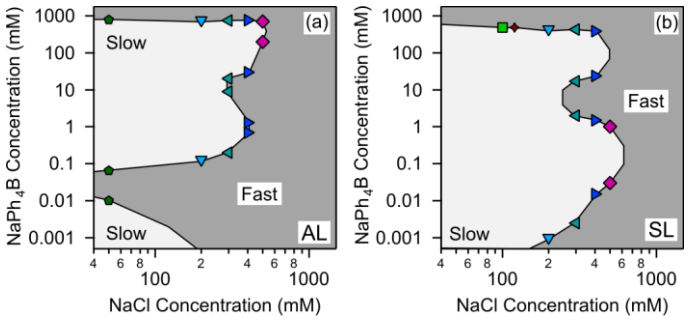

Figure 4. Stability maps of the $NaPh_4B$ concentration versus the NaCl concentration where the regions of slow and fast aggregation are separated by the CCC at pH 4.0. (a) Amidine latex, (b) sulfate latex.

Before discussing this unexpected effect further, let us address the dependence of the stability ratios for the SL particles on the Ph_4B^- concentration as shown in Fig. 3b. Without added NaCl, the particles aggregate extremely slowly, and fast aggregation is only observed than a very high Ph_4B^- concentrations. When NaCl is added, the aggregation behavior becomes more complicated. At very low Ph_4B^- concentrations, the stability ratios again reflect the behavior in pure NaCl solutions. The particles are stable at low NaCl concentrations, and with increasing NaCl concentration the stability ratio decreases again to unity. As the concentration of $NaPh_4B$ is increased, the stability ratio increases, most strongly at low NaCl concentration, but even at highest NaCl concentration of 500 mM investigated, an onset of this increase can be observed. This effect induces a CCC at low Ph_4B^- concentrations. We interpret this stabilization by the accumulation of additional negative charge on the negatively charged particles. This accumulation is caused by the adsorption of Ph_4B^- ions, and this effect could be also evidenced by electrophoresis. At very high concentrations of Ph_4B^-, near 500±10 mM, the stability ratio becomes unity again. This concentration marks again another CCC, above which one enters the fast aggregation region, where double layer forces are screened. The fast aggregation rates attained at high salt conditions are identical for NaCl and $NaPh_4B$ and for both types of particles within experimental error.

At intermediate concentrations of $NaPh_4B$ and NaCl, a similar unexpected effect as already mentioned for the AL particles occurs. This effect is more pronounced for SL than for AL, and now manifests itself most clearly as an intermediate minimum in the stability ratio around 10 mM. This minimum is measurable already at NaCl concentrations of 100 mM, but it becomes more prominent with increasing NaCl concentration. A stability ratio of unity is reached for NaCl concentrations above 300 mM, which leads to two additional CCCs. Furthermore, the existence of these CCCs leads to two intermediate maxima, and even at NaCl concentrations of 500 mM, one maximum is still present.

The four CCCs observed in our system can be rationalized as follow. The lowest CCC originates from the accumulation of negative charge on the SL particle through the adsorption of the Ph_4B^- anion. The highest CCC is due to screening of the double layer forces by salt. The two intermediate CCCs are caused by the presence of a further destabilization region, which must be caused by additional attractive non-DLVO interactions. A similar intermediate destabilization region can also be observed for AL particles.

A maximum similar to the ones shown in Fig. 3b was also reported in a like-charged systems, namely an anionic copolymeric latex in the presence of anionic surfactant, potassium stearate.[48] However, that study reports the maximum to occur at rather low concentrations of 0.3 mM extending only over a narrow concentration region. The authors interpret this maximum in terms of structural transition within the adsorbed surfactant film. Whether this maximum has the same origin than the ones reported here is currently unclear to us.

The stability maps shown in Fig. 4 clarify the effects of $NaPh_4B$ and NaCl on the aggregation of the AL and SL particles further. The maps show regions of slow and fast aggregation by plotting $NaPh_4B$ concentration versus the NaCl concentration, whereby the separating lines represent the CCCs.

Consider first the situation for AL particles shown in Fig. 4a. At low $NaPh_4B$ and NaCl concentrations, one observes a fast aggregation channel, which reflects the charge reversal. At high NaCl and $NaPh_4B$ concentrations, the aggregation is fast throughout due to screening. These effects generate the coastlines of the slow regions in the bottom of the map and the peninsula. The unexpected intermediate fast regime manifests itself as an indentation in the right hand side of the peninsula. Inspecting vertical cross-sections of this map, one finds three CCCs at low NaCl concentrations, but four CCCs around 300 mM NaCl.

The stability map for the SL particles shown in Fig. 4b is similar. Since the particles do not undergo a charge reversal, the fast channel is missing. Similarly to the AL particles after their charge reversal, the SL particles also increase the magnitude of their charge through the adsorption of the Ph_4B^- ions, which also results in a slow peninsula in the SL system. The indentation of the right hand side of the peninsula is again present, but is now more pronounced, and therefore the intermediate fast regime is larger. At low $NaPh_4B$ concentrations, one observes two CCCs, but again four CCCs in the regime of 300–400 mM NaCl.

DLVO calculations. We have first attempted to interpret the observed stability ratios with DLVO theory. Thereby, the interaction energies between charged interfaces were estimated by adding van der Waals and double layer contributions, and subsequently the interaction energy between the particles was estimated with the Derjaguin approximation. From these interaction energies, the aggregation rates were calculated by considering the diffusional motion of the particles. These rates

were subsequently normalized to obtain the stability ratio. The strength of van der Waals interaction was estimated with the Hamaker constant of 3.1×10^{-21} J, which was earlier used in similar calculations.[27] This value is very close to the ones extracted from direct force measurements between latex particles.[7,23]

The double layer force was obtained from the known concentration of monovalent salt and by approximating the diffuse layer potential by the electrokinetic potential (ζ-potential) as measured by electrophoresis. Thereby, the experimental values were interpolated by empirical fitting functions as shown in Fig. 2. Therefore, these calculations contain no adjustable parameters. Computational details can be found in the Experimental and Methods section.

The stability ratios calculated with DLVO theory are shown in Fig. 5. For AL particles, the calculations qualitatively reflect the observed stability patterns, see Fig. 5a. The minimum in the stability ratio near the neutralization point is reproduced rather well, as well as the sharp decrease of the stability ratio at high concentrations. DLVO theory correctly captures the upward shift of the highest CCC to 500–800 mM in $NaPh_4B$ solutions with respect to 150 mM in NaCl solutions (Table 1). Otherwise, however, the predictions lack accuracy. Especially, the DLVO theory fails to predict the experimentally observed intermediate minimum of the stability ratio around 10 mM. Moreover, the calculations predict a too strong dependence on the concentration, as evident from the too steep slopes of the calculated stability curves. Overall, DLVO theory suggests that the particles should be more stable than they actually are.

For the SL particles, the predictions of the DLVO theory reproduce the behavior of the stability ratios only at low and high Ph_4B^- concentrations, see Fig. 5b. These calculations demonstrate clearly that the increase in the stability ratio at low concentration is indeed due to the accumulation of negative charge on the particle surface due to adsorption of Ph_4B^-. The decrease in the stability ratio at high concentrations is also predicted, but this aspect is not surprising since double layer interactions will be always screened at sufficiently high salt concentrations.

The stability maps calculated with DLVO theory shown in Fig. 6 clarify the situation further. These maps were obtained by extracting the respective CCCs from the calculated stability profiles, and by plotting the respective $NaPh_4B$ concentration versus the NaCl concentration. The calculated stability maps reflect the measured ones reasonably well, especially for the AL particles. In this case, one finds the fast channel near the neutralization point as well the slow peninsula at higher $NaPh_4B$ concentrations. For the SL particles, the calculations correctly predict the existence of the slow peninsula. For both systems, however, the DLVO calculations fail to account for the fast indentations at the tip of the peninsula.

In the DLVO calculations discussed so far, constant potential (CP) boundary conditions were assumed. These boundary conditions correspond to substantial regulation of the surface charge approach, and this regulation would be caused by desorption of the Ph_4B^- anions. The other important boundary condition is the one with constant charge (CC). This condition assumes that the surface charge remains constant, and that no desorption upon approach takes place. We have thus compared the results of the calculations with these two boundary conditions. Since double layer forces with CC conditions are more repulsive than with CP conditions, the calculated stability ratios are higher. However, the generic features remain the same. This effect is particularly evident in the stability maps, where results obtained with CP and CC boundary conditions are compared. One should further note that more appropriate boundary conditions would lie in between CP and CC, but the consideration of more realistic boundary conditions will not influence these results substantially. Therefore, the origin of the intermediate destabilization region cannot be explained by different boundary conditions and must lie beyond DLVO theory.

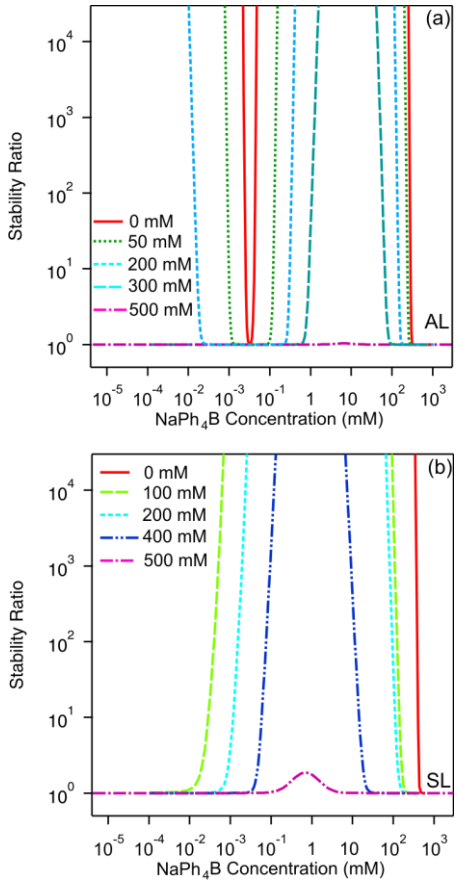

Figure 5. Stability ratios calculated with DLVO theory with constant potential (CP) boundary conditions versus the concentration of $NaPh_4B$ and different concentrations of added NaCl at pH 4.0. The diffuse layer potentials were approximated with the empirical fits of the electrokinetic potentials shown in Fig. 2. The Hamaker constant used was 3.1×10^{-21} J. (a) Amidine latex, (b) sulfate latex.

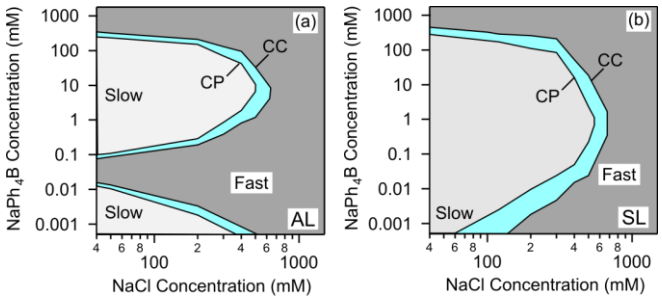

Figure 6. Stability maps of the $NaPh_4B$ concentration versus the NaCl concentration calculated with DLVO theory with constant potential (CP) and constant charge (CC) boundary conditions. Same parameters as in Fig. 5 were used. (a) Amidine latex, (b) sulfate latex.

Calculations including non-DLVO interactions. Various experiments based on direct force measurements have revealed that systems containing strongly adsorbing ions feature additional attractive non-DLVO forces.[7,23-25] In particular, such forces were also observed to act between sulfate latex and silica particles in the presence of Ph_4As^+ ions.[23] These forces can be fitted with the exponential law given in eq. (11) with a decay length around $q^{-1} = 3$ nm. The amplitude A of this force goes through a maximum versus the Ph_4As^+ concentration. Moreover, theoretical analysis suggests that additional attractive interactions between surfaces with a patch-charge distribution may occur and that such interactions decay exponentially.[31]

We suspect that similar non-DLVO forces are acting in the systems containing Ph_4B^- anions studied here. We thus use the decay length of 3 nm, and we empirically adjust the magnitude of the amplitude together with the position and the width of the maximum on the concentration axis, as shown in Fig. 7. The dependence of the amplitude A in eq. (11) on the concentration c of Ph_4B^- is thus modeled by the empirical expression

$$A = A_0 \exp\left[-\frac{\ln^2(c/c_0)}{2w}\right] \qquad (12)$$

where we use $w = 0.5$ for both types of particles. The maximum amplitude A_0 and the concentration c_0 at the peak are taken to be 0.16 mN/m and 7 mM for AL and 0.24 mN/m and 1 mM for SL. As illustrated in eq. (6), the additional interaction is added to the DLVO potential used previously, and the respective stability ratios are calculated in the same fashion again. The parameters were chosen such that the experimental stability data could be reproduced best. The width of the peak is similar to the one reported by Smith et al.[23] for Ph_4As^+, but the maximum amplitude chosen here is about 2–3 times larger. The latter study reported that this peak is positioned at charge neutralization point, but a similar peak was positioned way above this point in a system containing multivalent amine cations.[7] Note that this interaction is assumed not depend on the concentration of added NaCl.

The calculated stability ratios by including the non-DLVO interaction are shown in Fig. 8. The additional attractive non-DLVO force indeed induces an additional destabilization regime, which resembles the experimentally observed one. For both types of latex particles, the calculated stability ratios now feature four CCCs at certain NaCl levels, which is in accord with the experimental observations.

Clearly, the agreement is hardly quantitative. The predicted dependencies on the concentration are again too strong, which manifests in the large slopes in the calculated stability plots. Nevertheless, the asymmetries between the two intermediate maxima in the stability plots are reproduced by the calculations reasonably well.

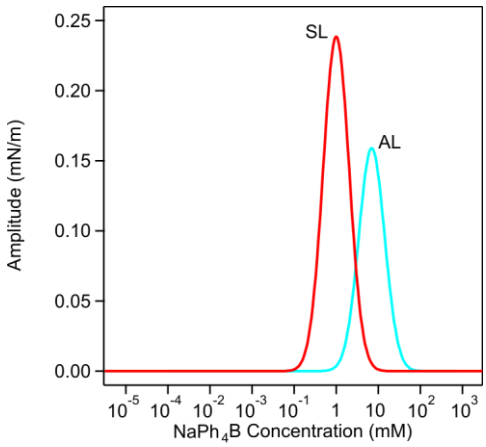

Figure 7. Dependence of the amplitude *A* used in eq. (11) on the concentration of of $NaPh_4B$ for the two types of latex particles.

The calculated stability maps including the non-DLVO interactions are shown in Fig. 9 and they reproduce the experimental maps surprisingly well. In particular, these maps now also show the characteristic fast indentations in the peninsulas, which is in full agreement with experiment. Therefore, we think that the calculations including the non-DLVO force, albeit not fully quantitative, reflect the essential features observed experimentally, and thus capture the mechanism of the aggregation process induced by the presence of Ph_4B^- anions for the AL as well as SL particles.

We thus strongly suspect that additional attractive non-DLVO interactions are responsible for the destabilization behavior observed at intermediate $NaPh_4B$ and NaCl concentrations. The strength of the non-DLVO interactions goes through a maximum as a function of the $NaPh_4B$ concentration, and these interactions appear similar to the ones, which were recently observed in direct force measurements between negatively charged surfaces in the presence of Ph_4As^+.[23] For this reason, we also suspect that their origin is similar. From the direct force measurements it was concluded that these forces are induced by surface charge heterogeneities, which are generated by the adsorption of

the hydrophobic ions. These heterogeneities are expected to occur in both AL and SL systems, since in the relevant region the adsorbed films will be rather dense, but defects in these films would induce the charge heterogeneities in question. These heterogeneities are expected to occur on a small length scales, probably the order of 1 nm, as one can estimate from the Debye length at the respective salt levels. However, charge fluctuations or hydrophobic interactions may contribute to these interactions as well.

Our parameterization of the additional non-DLVO interaction is admittedly crude. In particular, we assume that this force has no dependence on the presence of added NaCl, which is probably incorrect.[24] For the calculations of the stability ratios, however, this force is only relevant in a relatively narrow window of NaCl concentrations, and within this window the parameters used might indeed remain approximately constant. Nevertheless, more detailed studies would be necessary to characterize this additional force more fully. Our calculations of the stability ratios further suffer from a too strong concentration dependence, which overestimates the magnitudes of the slopes in the stability graphs. This shortcoming of the DLVO theory has been remarked already quite some time ago.[11,12,47,49] While surface charge heterogeneities have been proposed to be the origin of these discrepancies, it remains unclear how to include this effect into the stability calculations in a quantitative matter.

Conclusions

Electrophoretic mobility and aggregation rates are studied in aqueous suspensions of amidine latex (AL) and sulfate latex (SL) particles containing $NaPh_4B$ and NaCl. The hydrophobic Ph_4B^- anion is found to adsorb strongly, which leads to an accumulation of negative charge on both types of particles. This accumulation induces a region of slow aggregation, which is consistent with the classical DLVO theory. However, we observe an additional region of fast aggregation at intermediate concentrations. We argue that this fast aggregation region is caused by attractive non-DLVO forces, which are probably caused by surface charge heterogeneities within the adsorbed layer. While similar attractive forces were recently observed with direct force measurements[7,23,24], the present data are the first ones that demonstrate the importance of such attractive non-DLVO forces in particle aggregation. Further studies have to be carried out to find out to which extent the observed effects also occur for other types of hydrophonic ions, especially, for short-chain surfactants.

Acknowledgements

This research was supported by the Swiss National Science Foundation through projects no. 159874 and 178759 and the University of Geneva.

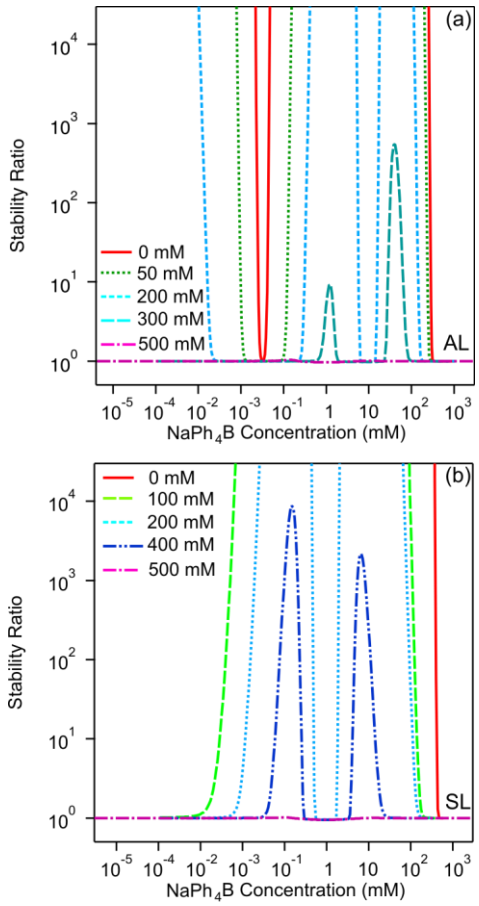

Figure 8. Stability ratios calculated by including the attractive non-DLVO interactions versus the concentration of $NaPh_4B$ and different concentrations of added NaCl at pH 4.0. The DLVO part of the calculations was the same as used in Fig. 5. (a) Amidine latex, (b) sulfate latex.

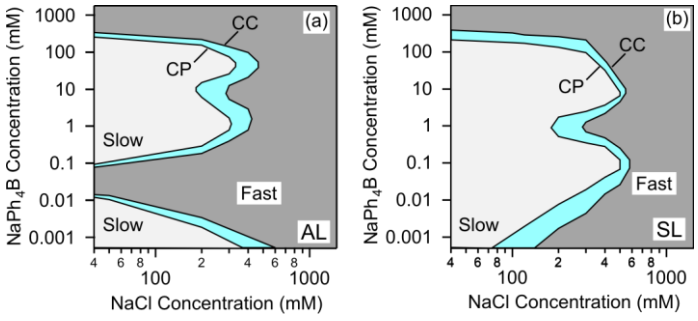

Figure 9. Stability maps of the $NaPh_4B$ concentration versus the NaCl concentration calculated by including the attractive non-DLVO interactions versus the concentration of $NaPh_4B$ and different concentrations of added NaCl at pH 4.0. The DLVO part of the calculations is the same used in Fig. 6. (a) Amidine latex, (b) sulfate latex.

References

1. Russel, W. B.; Saville, D. A.; Schowalter, W. R., *Colloidal Dispersions*. Cambridge University Press: Cambridge, 1989.
2. Elimelech, M.; Gregory, J.; Jia, X.; Williams, R. A., *Particle Deposition and Aggregation: Measurement, Modeling, and Simulation*. Butterworth-Heinemann Ltd.: Oxford, 1995.
3. Bolto, B.; Gregory, J., Organic Polyelectrolytes in Water Treatment. *Water Res.* **2007,** *41*, 2301-2324.
4. Horn, D.; Linhart, F., *Retention aids*. 2nd ed.; Blackie Academic and Professional: London, 1996.
5. Derjaguin, B.; Landau, L. D., Theory of the Stability of Strongly Charged Lyophobic Sols and of the Adhesion of Strongly Charged Particles in Solutions of Electrolytes. *Acta Phys. Chim.* **1941,** *14*, 633-662.
6. Verwey, E. J. W.; Overbeek, J. T. G., *Theory of Stability of Lyophobic Colloids*. Elsevier: Amsterdam, 1948.
7. Moazzami-Gudarzi, M.; Trefalt, G.; Szilagyi, I.; Maroni, P.; Borkovec, M., Forces between Negatively Charged Interfaces in the Presence of Cationic Multivalent Oligoamines Measured with the Atomic Force Microscope. *J. Phys. Chem. C* **2015,** *119*, 15482-15490.
8. Hartley, P. G.; Larson, I.; Scales, P. J., Electrokinetic and Direct Force Measurements between Silica and Mica Surfaces in Dilute Electrolyte Solutions. *Langmuir* **1997,** *13*, 2207-2214.
9. Wiese, G. R.; Healy, T. W., Coagulation and Electrokinetic Behavior of TiO_2 and Al_2O_3 Colloidal Dispersions. *J. Colloid Interface Sci.* **1975,** *51*, 427-433.
10. Frens, G.; Heuts, J. J. F. G., The Double Layer Potential as a Rate Determining Factor in the Coagulation of Electrocratic Colloids. *Colloids Surf.* **1988,** *30*, 295-305.
11. Schudel, M.; Behrens, S. H.; Holthoff, H.; Kretzschmar, R.; Borkovec, M., Absolute Aggregation Rate Constants of Hematite Particles in Aqueous Suspensions: A Comparison of Two Different Surface Morphologies. *J. Colloid Interface Sci.* **1997,** *196*, 241-253.
12. Behrens, S. H.; Christl, D. I.; Emmerzael, R.; Schurtenberger, P.; Borkovec, M., Charging and Aggregation Properties of Carboxyl Latex Particles: Experiments versus DLVO Theory. *Langmuir* **2000,** *16*, 2566-2575.
13. Szilagyi, I.; Polomska, A.; Citherlet, D.; Sadeghpour, A.; Borkovec, M., Charging and Aggregation of Negatively Charged Colloidal Latex Particles in Presence of Multivalent Polyamine cations. *J. Colloid Interf. Sci.* **2013,** *392*, 34-41.
14. Pavlovic, M.; Huber, R.; Adok-Sipiczki, M.; Nardin, C.; Szilagyi, I., Ion Specific Effects on the Stability of Layered Double Hydroxide Colloids. *Soft Matter* **2016,** *12*, 4024-4033.
15. Kobayashi, M.; Yuki, S.; Adachi, Y., Effect of Anionic Surfactants on the Stability Ratio and Electrophoretic Mobility of Colloidal Hematite Particles. *Colloid Surf. A* **2016,** *510*, 190-197.

16. Szabo, T.; Toth, V.; Horvath, E.; Forro, L.; Szilagyi, I., Tuning the Aggregation of Titanate Nanowires in Aqueous Dispersions. *Langmuir* **2015,** *31*, 42-49.
17. Barringer, E. A.; Bowen, H. K., High-Purity, Monodisperse TiO_2 Powders by Hydrolysis of Titanium Tetraethoxide 1. Synthesis and Physical Properties. *Langmuir* **1985,** *1*, 414-420.
18. Barringer, E. A.; Bowen, H. K., High-purity, Monodisperse TiO_2 Powders by Hydrolysis of Titanium Tetraethoxide 2. Aqueous Interfacial Electrochemistry and Dispersion Stability. *Langmuir* **1985,** *1*, 420-428.
19. Schwierz, N.; Horinek, D.; Netz, R. R., Reversed Anionic Hofmeister Series: The Interplay of Surface Charge and Surface Polarity. *Langmuir* **2010,** *26*, 7370-7379.
20. Calero, C.; Faraudo, J.; Bastos-Gonzalez, D., Interaction of Monovalent Ions with Hydrophobic and Hydrophilic Colloids: Charge Inversion and Ionic Specificity. *J. Am. Chem. Soc.* **2011,** *133*, 15025-15035.
21. Sugimoto, T.; Nishiya, M.; Kobayashi, M., Electrophoretic Mobility of Carboxyl Latex Particles: Effects of Hydrophobic Monovalent Counter-Ions. *Colloid Polym. Sci.* **2017,** *295*, 2405-2411.
22. Hakim, A.; Nishiya, M.; Kobayashi, M., Charge Reversal of Sulfate Latex Induced by Hydrophobic Counterion: Effects of Surface Charge Density. *Colloid Polym. Sci.* **2016,** *294*, 1671-1678.
23. Smith, A. M.; Maroni, P.; Borkovec, M., Attractive Non-DLVO Forces Induced by Adsorption of Monovalent Organic Ions. *Phys. Chem. Chem. Phys.* **2018,** *20*, 158-164.
24. Zohar, O.; Leizerson, I.; Sivan, U., Short Range Attraction between Two Similarly Charged Silica Surfaces. *Phys. Rev. Lett.* **2006,** *96*, 177802.
25. Dishon, M.; Zohar, O.; Sivan, U., Effect of Cation Size and Charge on the Interaction between Silica Surfaces in 1:1, 2:1, and 3:1 Aqueous Electrolytes. *Langmuir* **2011,** *27*, 12977-12984.
26. Cao, T.; Sugimoto, T.; Szilagyi, I.; Trefalt, G.; Borkovec, M., Heteroaggregation of Oppositely Charged Particles in the Presence of Multivalent Ions. *Phys. Chem. Chem. Phys.* **2017,** *19*, 15160 - 15171.
27. Sugimoto, T.; Cao, T.; Szilagyi, I.; Borkovec, M.; Trefalt, G., Aggregation and Charging of Sulfate and Amidine Latex Particles in the Presence of Oxyanions. *J. Colloid Interf. Sci.* **2018,** *524*, 456-464.
28. O'Brien, R. W.; White, L. R., Electrophoretic Mobility of a Spherical Colloidal Particle. *J. Chem. Soc. Farad. Trans. II* **1978,** *74*, 1607-1626.
29. Holthoff, H.; Schmitt, A.; Fernandez-Barbero, A.; Borkovec, M.; Cabrerizo-Vilchez, M. A.; Schurtenberger, P.; Hidalgo-Alvarez, R., Measurement of Absolute Coagulation Rate Constants for Colloidal Particles: Comparison of Single and Multiparticle Light Scattering Techniques. *J. Colloid Interface Sci.* **1997,** *192*, 463-470.
30. Xu, S. H.; Sun, Z. W., Progress in Coagulation Rate Measurements of Colloidal Dispersions. *Soft Matter* **2011,** *7*, 11298-11308.

31. Miklavic, S. J.; Chan, D. Y. C.; White, L. R.; Healy, T. W., Double Layer Forces between Heterogeneous Charged Surfaces. *J. Phys. Chem.* **1994,** *98*, 9022-9032.
32. Donaldson, S. H.; Royne, A.; Kristiansen, K.; Rapp, M. V.; Das, S.; Gebbie, M. A.; Lee, D. W.; Stock, P.; Valtiner, M.; Israelachvili, J., Developing a General Interaction Potential for Hydrophobic and Hydrophilic Interactions. *Langmuir* **2015,** *31*, 2051-2064.
33. Adamczyk, Z.; Jaszczolt, K.; Michna, A.; Siwek, B.; Szyk-Warszynska, L.; Zembala, M., Irreversible Adsorption of Particles on Heterogeneous Surfaces. *Adv. Colloid Interface Sci.* **2005,** *118*, 25-42.
34. Popa, I.; Papastavrou, G.; Borkovec, M., Charge Regulation Effects on Electrostatic Patch-Charge Attraction Induced by Adsorbed Dendrimers. *Phys. Chem. Chem. Phys.* **2010,** *12*, 4863-4871.
35. Santore, M. M.; Kozlova, N., Micrometer Scale Adhesion on Nanometer-scale Patchy Surfaces: Adhesion Rates, Adhesion Thresholds, and Curvature-Based Selectivity. *Langmuir* **2007,** *23*, 4782-4791.
36. Watanabe, A., Physico-Chemical Studies on Surface Active Agents. 2. The Coagulation of Positive Silver Iodide Sols by Anionic Surface Active Agents. *Bull. Inst. Chem. Res. Kyoto Univ.* **1960,** *38*, 179-215.
37. Ottewill, R. H.; Rastogi, M. C., The Stability of Hydrophobic Sols in the Presence of Surface-Active Agents 2. The Stability of Silver Iodide Sols in the Presence of Cationic Surface-Active Agents. *Trans. Faraday Soc.* **1960,** *56*, 866-879.
38. Somasundaran, P.; Fuerstenau, D. W.; Healy, T. W., Surfactant Adsorption at Solid-Liquid Interface: Dependence of Mechanism on Chain Length. *J. Phys. Chem.* **1964,** *68*, 3562-3566.
39. Liang, L.; Morgan, J. J., Chemical Aspects of Iron-Oxide Coagulation in Water: Laboratory Studies and Implications for Natural Systems. *Aquat. Sci.* **1990,** *52*, 32-55.
40. Goloub, T. P.; Koopal, L. K., Adsorption of Cationic Surfactants on Silica. Comparison of Experiment and Theory. *Langmuir* **1997,** *13*, 673-681.
41. Szilagyi, I.; Sadeghpour, A.; Borkovec, M., Destabilization of Colloidal Suspensions by Multivalent Ions and Polyelectrolytes: From Screening to Overcharging. *Langmuir* **2012,** *28*, 6211-6215.
42. Gregory, J., Rates of Flocculation of Latex Particles by Cationic Polymers. *J. Colloid Interface Sci.* **1973,** *42*, 448-456.
43. Kaya, A.; Yukselen-Aksoy, Y., Zeta Potential of Soils with Surfactants and its Relevance to Electrokinetic Remediation. *J. Hazard. Mater.* **2005,** *120*, 119-126.
44. White, B.; Banerjee, S.; O'Brien, S.; Turro, N. J.; Herman, I. P., Zeta-Potential Neasurements of Surfactant-Wrapped Individual Single-Walled Carbon Nanotubes. *J. Phys. Chem. C* **2007,** *111*, 13684-13690.

45. Lin, W.; Kobayashi, M.; Skarba, M.; Mu, C.; Galletto, P.; Borkovec, M., Heteroaggregation in Binary Mixtures of Oppositely Charged Colloidal Particles. *Langmuir* **2006,** *22*, 1038-1047.
46. Ortega-Vinuesa, J. L.; Martin-Rodriguez, A.; Hidalgo-Alvarez, R., Colloidal Stability of Polymer Colloids with Different Interfacial Properties: Mechanisms. *J. Colloid Interface Sci.* **1996,** *184*, 259-267.
47. Kihira, H.; Ryde, N.; Matijevic, E., Kinetics of Heterocoagulation 2. The Effect of the Discreteness of Surface Charge. *J. Chem. Soc. Faraday Trans.* **1992,** *88*, 2379-2386.
48. Zaccone, A.; Wu, H.; Lattuada, M.; Morbidelli, M., Correlation between Colloidal Stability and Surfactant Adsorption/Association Phenomena Studied by Light Scattering. *J. Phys. Chem. B* **2008,** *112*, 1976-1986.
49. Shulepov, S. Y.; Frens, G., Surface Roughness and Particle Size Effect on the Rate of Perikinetic Coagulation: Experimental. *J. Colloid Interface Sci.* **1996,** *182*, 388-394.